2009 American Control Conference
Hyatt Regency Riverfront, St. Louis, MO, USA
June 10-12, 2009

Design Fabrication of High-Precision Stage and Ultrahigh-speed Nanoscale Positioning

Koichi Sakata, Hiroshi Fujimoto, Atsushi Hara and Kazuaki Saiki

Abstract— **Motion control techniques are employed on nanoscale positioning in precision mechanical equipment, for example, NC machine tools, exposure systems, and so on. The advanced motion control techniques are based on the precise current control. However, speed-up of the precise current response has a serious limitation because of the carrier period of an inverter. In addition, the positional response has to be slower than the current response. In this paper, an experimental precision stage was designed and fabricated. Then, a novel ultrahigh-speed nanoscale positioning was achieved based on multirate PWM control. The positional error is in 100 nm. The positioning time is 2 ms which is only 20 times as long as the carrier period.**

I. INTRODUCTION

Digital control of servomotors has been researched actively thanks to high-speed switching of Pulse Width Modulation (PWM) inverter and improved arithmetic processing of digital signal processor (DSP). Nowadays, motion control techniques are employed on nanoscale positioning in precision mechanical equipment, for example, NC machine tools, exposure systems, and so on. Especially, the high-precision motion control is required to achieve nanoscale positioning for stages of exposure systems. There are many researches of high precision positioning of the stage [1], [2], [3], [4], and [5].

Then, the high-precision motion control is founded on precise current control of the motor. The performance of the current control is very important. However, speed-up of the precise current response has a serious limitation because of the carrier period of an inverter. In addition, the positional response has to be slower than the current response. There is a research that field programmable gate array (FPGA) is developed for motor drives to solve the problem of the limitation of the carrier period [6]. In the other way of approach with control technology, there are advantages of reduction of cost and switching loss.

The authors applied multirate PWM control for positioning of a servo motor [7]. Positioning in 20 ms is achieved by using DSP in the case that carrier period is 2 ms. It was difficult to shorten the positioning time because of limitation of the torque and the resolution of encoder.

This research was partially supported by the Ministry of Education, Science, Sports and Culture, Grant-in-Aid for Scientific Research, 18686036, 20686028.

K. Sakata and H. Fujimoto are with the Department of Electrical and Computer Engineering, Yokohama National University, Yokohama 240-8501, Japan. sakata@hfl.dnj.ynu.ac.jp & hfuji@ynu.ac.jp

A. Hara and K. Saiki are with Nikon Corporation, Yokohama 244-8533, Japan. Hara.Atsushi@nikonoa.net & saiki.kazu@nikon.co.jp

In this paper, an experimental precision stage was designed and fabricated. Then, a novel ultrahigh-speed nanoscale positioning was achieved based on multirate PWM control. The positional error is in 100 nm. The positioning time is 2 ms which is only 20 times as long as the carrier period.

The remainder of this paper is organized as follows. Section II explains the constitution, the design and the characteristics of Nano-stage which is the designed experimental precision stage. In Section III, multirate PWM positioning which is based on perfect tracking control (PTC) and PWM-hold is considered. In Section IV, experiments of feedback control and ultrahigh-speed nanoscale positoning are shown. Finally, conclusions are described in Section V.

II. NANO-STAGE

An experimental high-precision Stage was designed and fabricated to research ultrahigh-speed nanoscale positioning. The experimental stage is called 'Nano-stage' below.

A. Constitution of Nano-stage

Fig. 1 shows the overview of Nano-stage. Nano-stage driven by linear motor is the stage whose friction is almost zero because of using the air guide. Moreover, Nano-stage has two linear encoders to measure both the motor part which is a drive and the stage part which is a load. The resolution of the linear encoders is 1 nm/pulse respectively to achieve nanoscale positioning.

Then, Nano-stage can be switched to two modes of the rigid mode and the two-inertia mode. In the two-inertia mode, the motor and the stage parts are connected by leaf springs. Changing the leaf springs can change the resonance characteristic. Nano-stege is switched to the rigid mode because the motor and the stage parts are fixed by plates.

B. Design Fabrication of Nano-stage

Nano-stage was fabricated after parts and forms of the stage are defined by finite element (FEM) analyses as the plant characteristic of the two-inertia mode looks like an industrial large precision stage. Fig. 2 shows the results of FEM analyses.

C. Characteristics of Nano-stage

Pole-zero canceling proportional-integral current controller was designed for the current loop to be first-order system whose band frequency is 1 kHz. Table. I shows parameters of Nano-stage in the rigid mode. In the rigid mode, the frequency response

$$\frac{\dot{y}}{i^{ref}} = \frac{1}{\tau s + 1} \cdot \frac{1}{Ms + B} \tag{1}$$

978-1-4244-4524-0/09/$25.00 ©2009 AACC

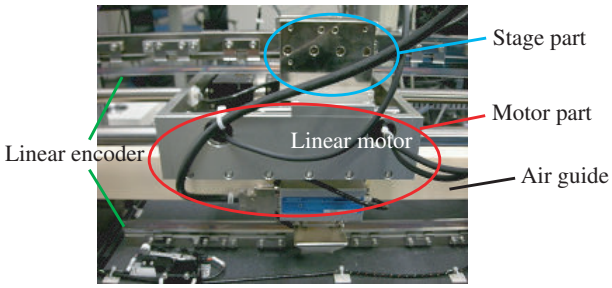

Fig. 1. Nano-stage.

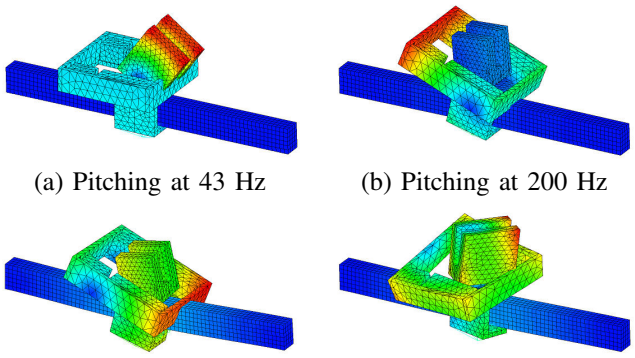

(a) Pitching at 43 Hz (b) Pitching at 200 Hz

(c) Pitching at 243 Hz (d) Twist at 400 Hz

Fig. 2. Finite element analyses.

TABLE I
PARAMETERS OF NANO-STAGE.

Inductance L	6.4	mH
Resistance R	13.1	Ω
Mass M	13.2	kg
Viscosity B	24.0	N/(m/s)
Thrust coefficient K_t	28.5	N/A
Back-emf constant K_e	9.5	V/(m/s)
Size	22×23×21	cm^3

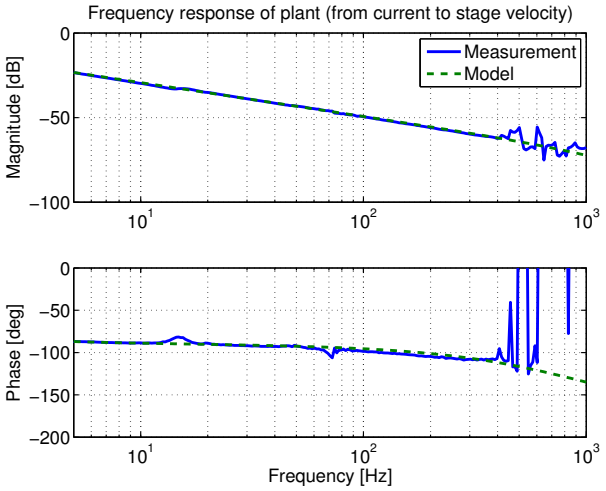

Fig. 3. Frequency response of rigid mode.

from the current reference to the velocity of the stage is shown in Fig. 3, where $\tau = 1/(2\pi 1000)$.

In the two-inertia mode, Fig. 4 and 5 show frequency responses of stage part and motor part respectively. 'Model' of broken line is the frequency response obtained by FEM analyses. In these figures, Nanostage could be fabricated, as it is almost the analysis.

III. MULTIRATE PWM POSITION CONTROL

Multirate PWM control system is a kind of perfect tracking control (PTC) system [8] which is designed for a plant model discretized based on PWM hold. In motion control, when position control systems of servomotors are designed, the dynamics of motors from the current to the position is regarded as a second-order plant without considering a current loop. However, the current loop cannot be ignored when the position loop system of bandwidth is higher and higher. Even if the current loop is modeled as the ideal first-order system, discretization errors remain in the control system because the current control system is designed as a digital control actually. In addition, when a motor is actuated by an inverter, the output voltage of the single-phase inverter can take only 0 or $\pm E$[V], and the output voltage of the three-phase inverter can take only 6 + 1 types of vectors. Therefore, a zero-order hold discretization causes modeling errors.

Multirate PWM control is designed considering a current loop and instantaneous values of PWM pulse precisely. High-speed positioning in some carrier sampling periods which are shorter than the response of the current loop can be achieved. In output voltage control of single-phase inverter, high performance control which is tracking the output voltage on an arbitrary waveform has been achieved [9].

A. Descrete Model Based on PWM-hold

In order to discretize a plant model, a zero-order hold is applied generally. However, in the case that a single-phase inverter (or a four-quadrant chopper) of Fig. 6 actuates DC-motor, the inverter can output not arbitrary output vector $V[k]$ but only 0 or $\pm E$[V] as Fig. 7. Therefore, in order to control instantaneous values precisely, the zero-order hold is unsuitable because the precise discrete model is based on the PWM hold of Fig. 7. The plant model of a motor actuated by an inverter can be discretized based on the PWM hold as follows [10].

A continuous-time state equation of a plant is represented by

$$\begin{cases} \dot{\boldsymbol{x}}(t) = \boldsymbol{A}_c\boldsymbol{x}(t) + \boldsymbol{b}_c u(t) \\ y(t) = \boldsymbol{c}_c\boldsymbol{x}(t) \end{cases} . \tag{2}$$

The precise discrete model in which the input $u[k]$ is the switching time $\Delta T[k]$. is obtained as

$$\begin{cases} \boldsymbol{x}[k+1] = \boldsymbol{A}_s\boldsymbol{x}[k] + \boldsymbol{b}_s\Delta T[k] \\ y[k] = \boldsymbol{c}_s\boldsymbol{x}[k] \end{cases} . \tag{3}$$

$$\boldsymbol{A}_s = e^{\boldsymbol{A}_c T_u} \ , \ \boldsymbol{b}_s = e^{\boldsymbol{A}_c T_u/2}\boldsymbol{b}_c E \ , \ \boldsymbol{c}_s = \boldsymbol{c}_c$$

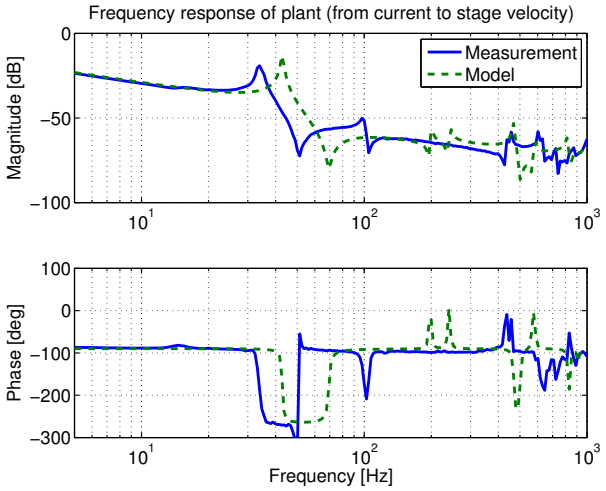

Fig. 4. Frequency response of stage part.

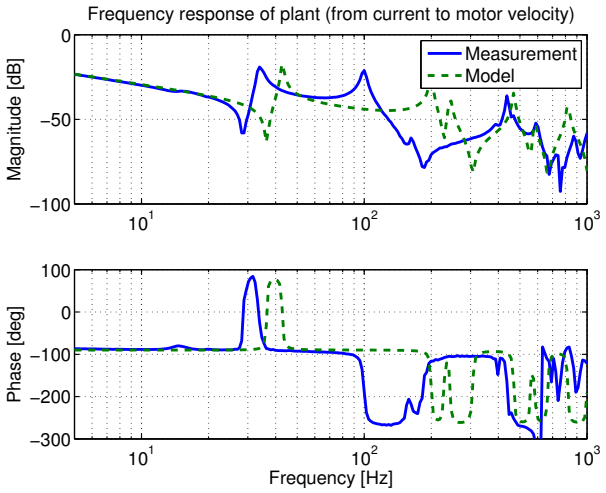

Fig. 5. Frequency response of motor part.

When $\Delta T[k]$ is negative, $-E$[V] is outputted. (3) can be applied for AC-servo system driven by 3-phase inverter with vector control [7].

B. Perfect Tracking Control

Perfect tracking control (PTC) which consists of the 2-DOF control system as shown in Fig .8. This system has two samplers for the reference signal $r(t)$ and the output $y(t)$, and one holder for the input $u(t)$. Therefore, there exist sampling periods T_r, T_y, and T_u which represent the periods of $r(t)$, $y(t)$, and $u(t)$, respectively. PTC applies the multirate feedforward control in which the control input $u(t)$ is changed n times during one sampling period T_r of reference input $r(t)$ as shown in Fig. 9. Here, n is the plant order. H_M in Fig. 8 is the multirate holder which outputs the input $u[i] = [u_1[k], \cdots, u_n[k]]^T$ (generated by the long sampling period T_r) on the short sampling period T_u.

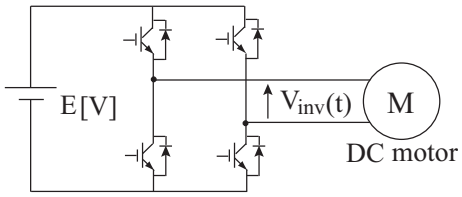

Fig. 6. Single-phase inverter.

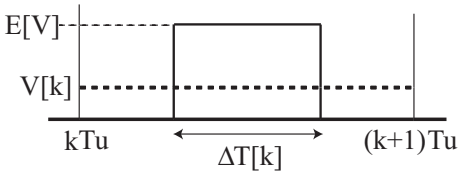

Fig. 7. PWM hold.

Here, the matrices $\boldsymbol{A}$, $\boldsymbol{B}$, $\boldsymbol{C}$ and $\boldsymbol{D}$ are given as

$$\left[\begin{array}{c|c}\boldsymbol{A} & \boldsymbol{B}\\ \hline \boldsymbol{C} & \boldsymbol{D}\end{array}\right]=\left[\begin{array}{c|cccc}\boldsymbol{A}_s^n & \boldsymbol{A}_s^{n-1}\boldsymbol{b}_s & \cdots & \boldsymbol{A}_s\boldsymbol{b}_s & \boldsymbol{b}_s\\ \hline \boldsymbol{c}_s & 0 & \cdots & 0 & 0\\ \boldsymbol{c}_s\boldsymbol{A}_s & \boldsymbol{c}_s\boldsymbol{b}_s & \cdots & 0 & 0\\ \vdots & \vdots & \ddots & \vdots & \vdots\\ \boldsymbol{c}_s\boldsymbol{A}_s^{n-1} & \boldsymbol{c}_s\boldsymbol{A}_s^{n-2}\boldsymbol{b}_s & \cdots & \boldsymbol{c}_s\boldsymbol{b}_s & 0\end{array}\right] \quad (4)$$

by (3). Since the matrix $\boldsymbol{B}$ of (4) is non-singular. PTC can be designed as

$$\begin{aligned}\boldsymbol{u}_0[i] &= \boldsymbol{B}^{-1}(\boldsymbol{I}-z^{-1}\boldsymbol{A})\boldsymbol{x}_d[i+1]\\ &= \left[\begin{array}{c|c}\boldsymbol{0} & \boldsymbol{I}\\ \hline -\boldsymbol{B}^{-1}\boldsymbol{A} & \boldsymbol{B}^{-1}\end{array}\right]\boldsymbol{x}_d[i+1] \quad (5)\\ y_o[i] &= z^{-1}\boldsymbol{C}\boldsymbol{x}_d[i+1]+\boldsymbol{D}\boldsymbol{u}_0[i]. \quad (6)\end{aligned}$$

(5) is the stable inverse system of plant as the references are state variables $\boldsymbol{x}_d[k+1]$. Therefore, the perfect tracking is assured on the sampling period T_r .

Moreover, The feedback control $C_2[z]$ suppresses the error between the output $y[k]$ and the nominal output $y_0[k]$ to assure robustness only when disturbances or plant variations exist.

C. Original PTC system

PTC is designed for the third-order plant as the current loop is the ideal first-order system. This method is named 'Conventional 2'. The design method for the second-order plant ignored current loop is named 'Conventional 1'.

The plant of Conventional 1 is described by

$$\frac{y}{i^{ref}}=\frac{1}{Ms^2+Bs}. \quad (7)$$

The plant of Conventional 2 is described by

$$\frac{y}{i^{ref}}=\frac{1}{\tau s+1}\cdot\frac{1}{Ms^2+Bs}. \quad (8)$$

These plants are discretized by zero-order hold, then PTC is designed.

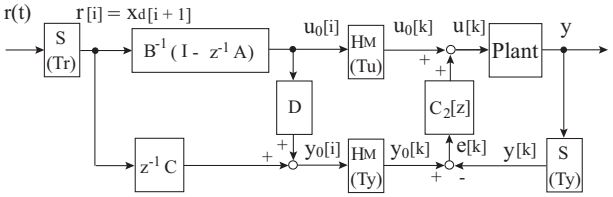

Fig. 8. Perfect tracking control system.

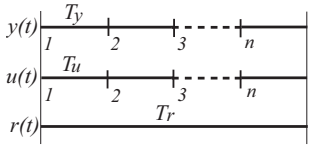

Fig. 9. Multirate sampling period.

D. Constitution of Multirate PWM Position Control System

In the rigid mode, q axis model of Nano-stage is shown in 10. Therefore, a control system can be designed for the model with a vector control. The transfer function from V_{inv} to y is described by

$$\frac{y}{V_{inv}} = \frac{K_t}{MLs^3 + (MR + LB)s^2 + (BR + K_e K_t)s}. \tag{9}$$

The controllable canonical form of (9) is given by

$$\dot{\boldsymbol{x}}(t) = \boldsymbol{A}_c \boldsymbol{x}(t) + \boldsymbol{b}_c u(t) \ , \ y(t) = \boldsymbol{c}_c \boldsymbol{x}(t), \tag{10}$$

$$\left[\begin{array}{c|c} \boldsymbol{A}_c & \boldsymbol{b}_c \\ \hline \boldsymbol{c}_c & 0 \end{array}\right] = \left[\begin{array}{ccc|c} 0 & 1 & 0 & 0 \\ 0 & 0 & 1 & 0 \\ 0 & -\frac{BR+K_eK_t}{ML} & -\frac{MR+LB}{ML} & \frac{K_t}{ML} \\ \hline 1 & 0 & 0 & 0 \end{array}\right], \tag{11}$$

where $\boldsymbol{x} = [\ y \ \ \dot{y} \ \ \ddot{y}\ ]^T$.

Also, the transfer function from V_{inv} to i is described by

$$\frac{i}{V_{inv}} = \frac{Ms^2 + Bs}{MLs^3 + (MR + LB)s^2 + (BR + K_e K_t)s}. \tag{12}$$

The output equation of (12) is represented by

$$y = \boldsymbol{c}_c' \boldsymbol{x} \ , \ \boldsymbol{c}_c' = \left[\ 0 \quad \frac{B}{K_t} \quad \frac{J}{K_t}\ \right]. \tag{13}$$

The multirate PWM position control system considering PWM hold can be designed as Fig. 11. The current controller $C_{PI}[z]$ and the position controller $C_2[z]$ operate only when the errors between the nominal outputs and the actual outputs exist.

IV. EXPERIMENTS

In the rigid mode, experiments were performed. A feedback controller was designed for the steady-state position error to be as small as possible in nanoscale. Then, experiments of ultrahigh-speed nanoscale positioning with multirate PWM control were performed.

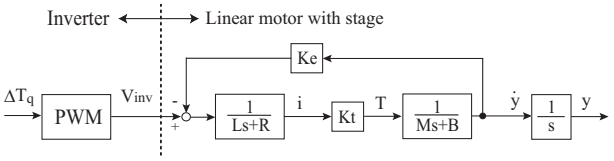

Fig. 10. q axis model of rigid mode.

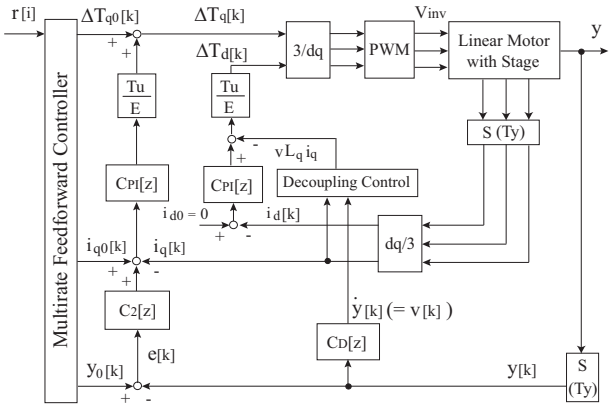

Fig. 11. Multirate PWM positional control system.

A. Design of Feedback Control

A proportional-integral-derivative position controller was designed, as band frequency of the position loop is 100 Hz. Fig. 13 shows the steady-state position error with the feedback controller. In the spectrum of the position error, the peak exists at 75 Hz. It seems to be caused by input disturbance via the structure of Nano-stage.

Therefore, a peak filter was inserted in the position controller. The peak filter was designed for the sensitivity characteristic of Fig. 12. Fig. 14 shows the steady-state position error with the peak filter. The standard deviation 3σ of the steady-state position error can be suppressed in 81 nm.

B. Ultrahigh-speed Nanoscale Positioning

In the specification of Table. II, experiments of ultrahigh-speed nanoscale positioning. In the table, t_d is the positioning time, and A^{ref} is the target position. The target position trajectory is based on a 5-order polynomials. Here, position error tolerance is defined as 100 nm from the preceding section. The multirate PWM position control was compared with original PTC based on the discrete model by zero-order hold.

Fig. 15 and 16 show the experimental results of Spec. 1 and Spec. 2 respectively. In spec. 1 of 10 ms positioning, the errors of all methods are suppressed in the position error tolerance at the positioning time. In spec. 2 of 2 ms positioning, the errors of original PTC systems are not suppressed in the position error tolerance at the positioning time. On the other hands, the multirate PWM position control achieves the target specification.

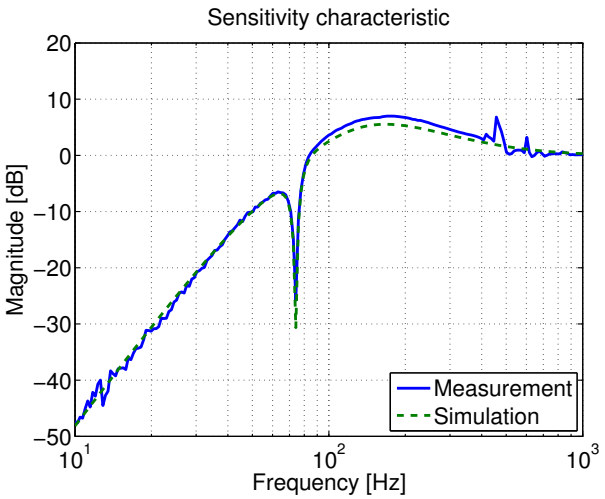

Fig. 12. Sensitivity characteristic.

TABLE II

SAMPLING PERIODS AND TARGET TRAJECTORY.

	T_u	T_y	t_d	A^{ref}
Spec. 1	0.1 ms	0.1 ms	10 ms	1 μm
Spec. 2	0.1 ms	0.1 ms	2 ms	1 μm

V. CONCLUSIONS

In this paper, precision stage was designed and fabricated for nanoscale positioning. In the rigid mode, multirate PWM position control system was structured. Then, a novel ultrahigh-speed nanoscale positioning was achieved. The positional error is in 100 nm. The positioning time is 2 ms which is only 20 times as long as the carrier period.

In future works, ultrahigh-speed nanoscale positioning of the two-inertia mode will be tried to apply the technique for precision mechanical equipment, for example, NC machine tools, exposure systems, and so on.

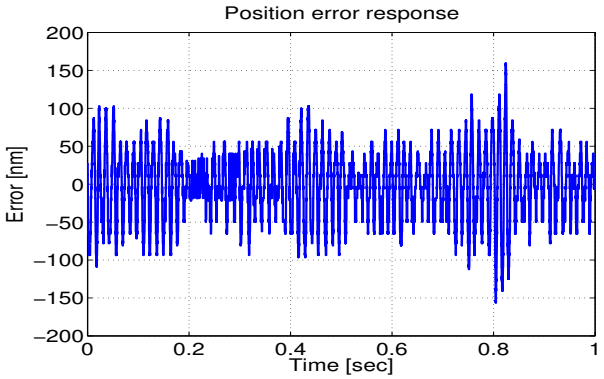

(a) Time response

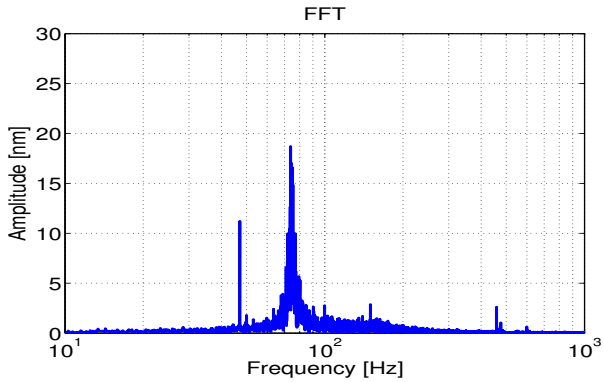

(b) Spectrum

Fig. 13. Steady-state position error w/o peak-filter.

REFERENCES

[1] R. A. de Callafon and P. M. J. Van den Hof, "Multivariable Feedback Relevant System Identification of a Wafer Stepper System", *IEEE Trans. Control System Technology*, vol. 9, no. 2, pp. 381–390, 2001.

[2] M. van de Wal, G. van Baars, F. Sperling, and O. H. Bosgra, "Multivariable $\mathcal{H}_\infty/\mu$ feedback control design for high-precision wafer stage motion", *Control Engineering Practice*, vol. 10, issue 7, pp. 739–755, 2002.

[3] C. L. van Oosten, O. H. Bosgra, and B. G. Dijkstra, "Reducing residual vibrations through Iterative Learning Control, with application to a wafer stage", in *Proc. American Control Conference*, pp. 5150–5155, 2004.

[4] M. Heertjes and N. van de Wouw, "Variable Control Design and its Application to Wafer Scanners", in *Proc. Conference on Decision and Control*, pp. 3724–3729, 2006.

[5] S. H. van der Meulen, R. L. Tousain, and O. H. Bosgra, "Fixed Structure Feedforward Controller Design Exploiting Iterative Trials: Application to a Wafer Stage and a Desktop Printer", *Journal of Dynamic Systems, Measurement and Control*, vol. 130, 051006-1/16, 2008.

[6] T. Yokoyama, M. Horiuchi, S. Simogata, "Instantaneous Deadbeat Control for PWM Inverter Using FPGA Based Hardware Controller", in *Proc. IECON'03*, vol. 1, pp. 180–185, 2003.

[7] K. Sakata, and H. Fujimoto, "Perfect Tracking Control of Servo Motor Based on Precise Model with PWM Hold and Current Loop", in *Proc. The Fourth Power Conversion Conference*, pp. 1612–1617, 2007.

[8] H. Fujimoto, Y. Hori, and A. Kawamura, "Perfect Tracking Control based on Multirate Feedforward Control with Generalized Sampling Periods", *IEEE Trans. Industrial Electronics*, vol. 48, no. 3, pp. 636–644, 2001.

[9] H. Abe and H. Fujimoto, "Multirate Perfect Tracking Control of Single-phase Inverter with Inter Sampling for Arbitrary Waveform", in *Proc. The Fourth Power Conversion Conference*, pp. 810–815, 2007.

[10] K. P. Gokhale, A. Kawamura, and R. G. Hoft, "Deat Beat Microprocessor Control of PWM Inverter for Sinusoidal Output Waveform Synthesis", *IEEE Trans. Industry Applications*, vol. 23, no. 3, pp. 901–910, 1987.

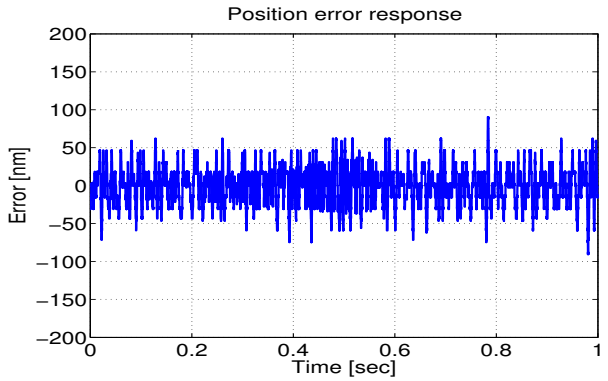

(a) Time response

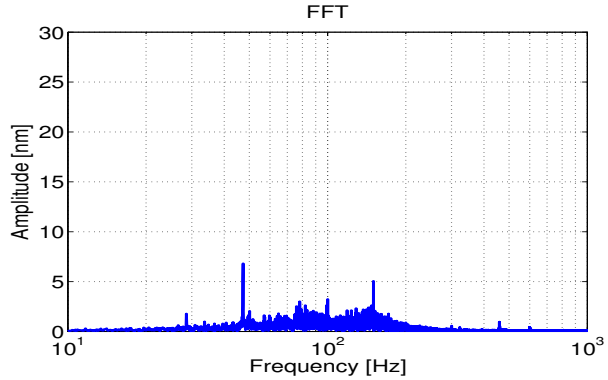

(b) Spectrum

Fig. 14. Steady-state position error with peak-filter.

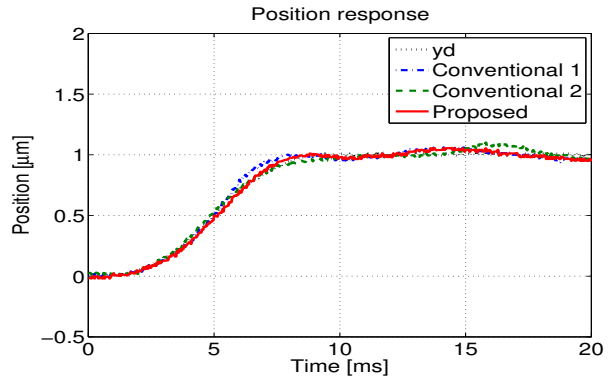

(a) Position response

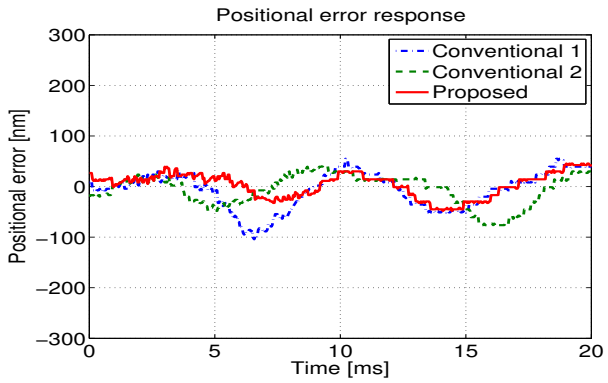

(b) Positional error response

Fig. 15. Experimental result of PTC in Spec. 1.

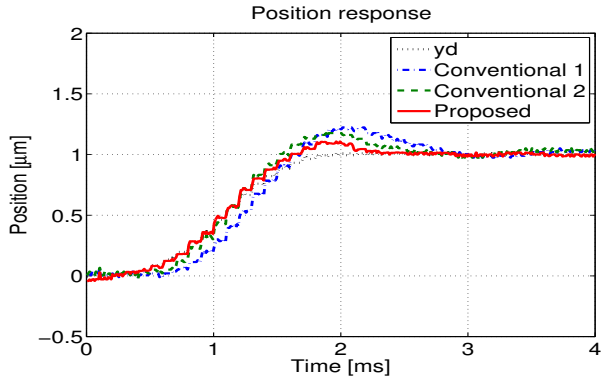

(a) Position response

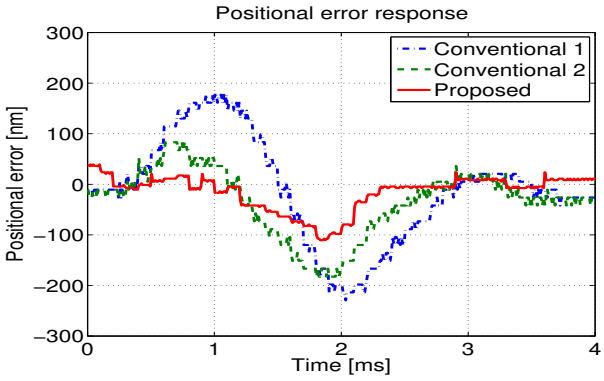

(b) Positional error response

Fig. 16. Experimental result of PTC in Spec. 2.